Journal of Power Sources 195 (2010) 2900–2904

Contents lists available at ScienceDirect

Journal of Power Sources

journal homepage: www.elsevier.com/locate/jpowsour

Short communication

A novel layered material of $LiNi_{0.32}Mn_{0.33}Co_{0.33}Al_{0.01}O_2$ for advanced lithium-ion batteries

Feng Wu[a,b], Meng Wang[a,b], Yuefeng Su[a,b,*], Liying Bao[a,b], Shi Chen[a,b]

[a] School of Chemical Engineering and Environment, Beijing Institute of Technology, Beijing 100081, China
[b] National Development Center of High Technology Green Materials, Beijing 100081, China

ARTICLE INFO

Article history:
Received 19 May 2009
Received in revised form 8 September 2009
Accepted 10 November 2009
Available online 14 November 2009

Keywords:
Cathode material
Al substitution
Li-ion battery
Cycling performance

ABSTRACT

A novel layered material of $LiNi_{0.32}Mn_{0.33}Co_{0.33}Al_{0.01}O_2$ with α-$NaFeO_2$ structure is synthesized by sol–gel method. X-ray diffraction (XRD) shows that the cation mixing in the Li layers of it is decreased. In addition, cyclic voltammetry (CV) and electrochemical impedance spectroscopy (EIS) are employed to characterize the reaction of lithium-ion insertion and extraction from materials. The results indicate that the structure of $LiNi_{0.32}Mn_{0.33}Co_{0.33}Al_{0.01}O_2$ is more stable than that of the $LiNi_{0.33}Mn_{0.33}Co_{0.33}O_2$. The capacity retention of $LiNi_{0.33}Mn_{0.33}Co_{0.33}O_2$ after 40 cycles at 2.0 C is only 89.9%, however, that of the $LiNi_{0.32}Mn_{0.33}Co_{0.33}Al_{0.01}O_2$ is improved to 97.1%. The capacity of the $LiNi_{0.32}Mn_{0.33}Co_{0.33}Al_{0.01}O_2$ at 4.0 C remains 71.8% of the capacity at 0.2 C, while that of the $LiNi_{0.33}Mn_{0.33}Co_{0.33}O_2$ is only 54.3%. EIS measurement reveals that the increase in the charge transfer resistance during cycling is suppressed in the $LiNi_{0.32}Mn_{0.33}Co_{0.33}Al_{0.01}O_2$ material.

1. Introduction

Since Ohzuku and Makimura [1] first proposed a layered compound $LiNi_{0.33}Mn_{0.33}Co_{0.33}O_2$, it has attracted significant attention as a promising cathode material. It has high capacity, structural and thermal stability, and excellent cycle performance [2–5]. However, many problems still remained, such as low rate capability and considerable capacity loss at high current density. Many authors suggested that partial substitution for transition metal was an effective method in modifying the electronic structure and improving the electrochemical performances [6–9]. It is reported that Fe and Mg substitute for Ni in $LiNi_{1/3-x}Fe_xCo_{1/3}Mn_{1/3}O_2$ [10] and $LiNi_{0.6-x}Mg_xCo_{0.25}Mn_{0.15}O_2$ [11] could reduce the cation mixing, improve structural integrity and cycle stability. Obviously, substitute for Ni in the Ni-based oxide is appeared to be a good method to modify the structural and electrochemical performance of these materials. In this study, we employed aluminum (Al^{3+}) as a dopant due to the more negative Gibbs free energies of the Al_2O_3 [$\Delta_f G^{\theta}_{Al_2O_3} = -1582.3\ kJ\ mol^{-1}$] compares to that of NiO [$\Delta_f G^{\theta}_{NiO} = -211.7\ kJ\ mol^{-1}$] [12]. It is reasonable to deduce that the bonding energy of Al–O is much stronger than that of Ni–O. Therefore, by substituting a part of Ni with Al in layered $LiNi_{0.33}Mn_{0.33}Co_{0.33}O_2$, the total metal–oxygen bonding of the doped material is stronger than that of undoped one. Hence, we synthesized a novel layered material of $LiNi_{0.32}Mn_{0.33}Co_{0.33}Al_{0.01}O_2$ by substitute a small amount of Ni^{2+} in $LiNi_{0.33}Mn_{0.33}Co_{0.33}O_2$ with Al^{3+}. The structure and electrochemical properties of the compounds are investigated in this paper.

2. Experimental

$LiNi_{0.33-x}Mn_{0.33}Co_{0.33}Al_xO_2$ ($x = 0$, 0.01) materials were prepared by a sol–gel method using citric acid as a chelating agent. Stoichiometric amounts of $CH_3COOLi{\cdot}2H_2O$, $(CH_3COO)_2Ni{\cdot}4H_2O$, $(CH_3COO)_2Mn{\cdot}4H_2O$, $(CH_3COO)_2Co{\cdot}4H_2O$ and $Al(NO_3)_3{\cdot}9H_2O$ were dissolved in deionized water. The dissolved solutions were added drop by drop into the continuously agitated aqueous solution of citric acid. The metal:chelating agent was fixed to be 1:2. The pH of the solution was adjusted in the range of 7.0–9.0 by using ammonium hydroxide. Then the prepared solution was evaporated at 70–80 °C. The resulting precursors were heated with a heating rate of 5 °C min^{-1} and decomposed at 500 °C for 5 h in air. The powders were calcined at 850 °C for 16 h in air and then the sample was cooled slowly in the furnace to room temperature.

XRD measurement was carried out using a D Max-RD12Kw diffractometer with a Cu target Kα radiation. The scan data were collected in the 2θ range of 10–90° in steps of 1° min^{-1}. Scanning electron microscope (SEM) was performed using QUANTA 600. The Li, Ni, Mn, Co and Al contents in the samples were analyzed by

* Corresponding author at: School of Chemical Engineering and Environment, Beijing Institute of Technology, Beijing 100081, China. Tel.: +86 10 68918099; fax: +86 10 68918099.
E-mail address: suyuefeng@bit.edu.cn (Y. Su).

0378-7753/$ – see front matter © 2009 Elsevier B.V. All rights reserved.
doi:10.1016/j.jpowsour.2009.11.041

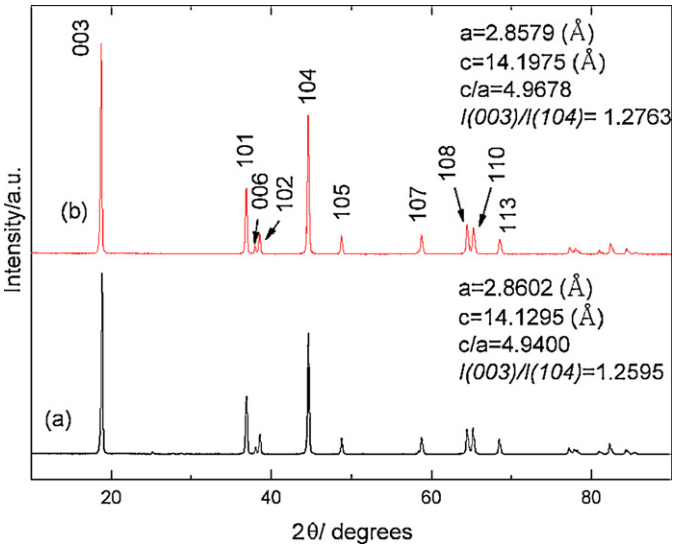

Fig. 1. X-ray diffraction patterns of the $LiNi_{0.33-x}Mn_{0.33}Co_{0.33}Al_xO_2$ powders: (a) $x = 0$ and (b) $x = 0.01$.

an inductively coupled plasmas spectrometer (ICP, IRIS Intrepid II XSP).

The electrochemical properties of $LiNi_{0.33-x}Mn_{0.33}Co_{0.33}Al_xO_2$ were examined in the CR2025 coin type cells. The cathode electrodes were prepared by pasting the mixture of 85.0 wt.% $LiNi_{0.33-x}Mn_{0.33}Co_{0.33}Al_xO_2$, 10.0 wt.% acetylene black and 5.0 wt.% PVDF onto a aluminum foil current collector. The electrolyte was 1 M $LiPF_6$/EC + DMC (1:1 in volume). The cells were assembled in an argon-filled glove box, then aged for 12 h before electrochemically cycled between 2.8 and 4.5 V (versus Li/Li^+) using CT2001A Land instrument.

The cyclic voltammogram (CV) was operated at 0.1 mV s^{-1} between 2.5 and 4.8 V. The electrochemical impedance spectroscopy (EIS) measurements were conducted by a CHI660a impedance analyzer, using an amplitude voltage 5 mV and frequency range was 0.001–0.1 MHz.

3. Results and discussion

3.1. X-ray diffraction and morphology

The XRD patterns of the $LiNi_{0.33-x}Mn_{0.33}Co_{0.33}Al_xO_2$ ($x = 0$, 0.01) materials are shown in Fig. 1. There is no impurity phase detected in the patterns, which indicates that a single phase layered $LiNi_{0.33-x}Mn_{0.33}Co_{0.33}Al_xO_2$ is obtained. The patterns also show clear split of the (0 0 6)/(1 0 2) and (1 0 8)/(1 1 0) peaks, indicating both the compounds have a high degree of ordered hexagonal structure [12]. The lattice parameters inserted in Fig. 1 were calculated by a least square method from the XRD patterns. The lattice parameter a indicates the metal-metal interlayer distance while c represents the interlayer spacing. It could see that the a parameter slightly decreases while the c parameter greatly increases. The incorporation of the smaller and more polarizing Al^{3+} ion ($r_{Al^{3+}} = 53.5$ pm [13]) in place of the larger Ni^{2+} ion ($r_{Ni^{2+}} = 69$ pm [13]) is the reason for the decreases of a [14]. The increases of c parameter could due to the polarizing effect of the Al^{3+} ion in the [MO_2] layers, which will to distort the structure and increase the interlayer distance along c-axis [15]. The variation in measured lattice parameters is in good agreement with those reported previously [16,17]. The increases of c-axis will provide an increase of chemical diffusion coefficients of Li^+ ions in $LiNi_{0.32}Mn_{0.33}Co_{0.33}Al_{0.01}O_2$. Moreover, c/a ratios of both samples are greater than 4.9, a value is well known for the material with layered characteristics. However, the c/a ratio of the sample $LiNi_{0.32}Mn_{0.33}Co_{0.33}Al_{0.01}O_2$ is larger than that of undoped one. It means the Al-doped sample has the higher layer properties and lower cation mixing [18,19]. The intensity ratio of (0 0 3)/(1 0 4) peaks is a sensitive parameter to determine the cation distribution in the lattice and the higher this ratio, the lower degree of the cation mixing [20,21]. Obviously, the $I_{(003)}/I_{(104)}$ value of $LiNi_{0.32}Mn_{0.33}Co_{0.33}Al_{0.01}O_2$ is higher than that of $LiNi_{0.33}Mn_{0.33}Co_{0.33}O_2$ which means the cation mixing in Li layer seemed to be decreased by Al^{3+} substitution. These observations are similar to the literature [22]. The increased c-axis and reduced cation mixing could consequently effect on the improvement on its rate capacity and cycling performance.

Fig. 2 shows the SEM photographs for $LiNi_{0.33-x}Mn_{0.33}Co_{0.33}Al_xO_2$ powders. The average particle size is about 100–500 nm, and there is no great difference between the $LiNi_{0.32}Mn_{0.33}Co_{0.33}Al_{0.01}O_2$ and $LiNi_{0.33}Mn_{0.33}Co_{0.33}O_2$. ICP was employed to measure the final elements ration in the samples. The atom ratio of Li:Ni:Mn:Co in the $LiNi_{0.33}Mn_{0.33}Co_{0.33}O_2$ sample is determined to be 1.003:0.335:0.331:0.334 by ICP emission spectrometry; while the atom ratio of Li:Ni:Mn:Co:Al in the $LiNi_{0.32}Mn_{0.33}Co_{0.33}Al_{0.01}O_2$ is determined to be 1.025:0.321:0.330:0.332:0.010. The results show that the chemical compositions of both samples are nearly equal to the stoichiometric ratio as decided.

3.2. Electrochemical behavior

Fig. 3 shows the initial charge–discharge curves for the $LiNi_{0.33-x}Mn_{0.33}Co_{0.33}Al_xO_2$ cells at a current density of 0.12 C (20 mA g^{-1}). The initial charged and discharge capacity of the $LiNi_{0.33}Mn_{0.33}Co_{0.33}O_2$ is about 209.9 and 177.6 mAh g^{-1}, respectively. A little decrease in the capacity is observed for the material of $LiNi_{0.32}Mn_{0.33}Co_{0.33}Al_{0.01}O_2$, which is 203.5 and 175.5 mAh g^{-1}. One of the reasons is that electrochemically inactive Al^{3+} substitution for active Ni^{2+} ions could decrease the amount of Ni^{2+}/Ni^{4+} reaction. However, it could see that the coulombic efficiency is improved from 84.6% to 86.2% after doping. Delmas et al. [23,24] ascribed an irreversible loss of capacity between the first charge and first discharge to the formation of electrochemically inactive regions in the cathode due to the oxidation of pre-existing Ni^{2+} ions which occupy the Li layer. The improved coulombic efficiency is related to the suppressed cation mixing in the doped material. For the Al^{3+}-doped sample, the cation mixing in the Li layer is suppressed effectively so that Li^+ ions will be less blocked by Ni^{2+} ions, resulting in highly reversible Li^+ intercalation/deintercalation during cycling.

Fig. 4 shows the cycling performance of the $LiNi_{0.33-x}Mn_{0.33}Co_{0.33}Al_xO_2$ cells at 2.0 C current. Although the $LiNi_{0.33}Mn_{0.33}Co_{0.33}O_2$ delivered a discharge capacity of 115.5 mAh g^{-1} for first cycle, it suffered a severe capacity fading and reaches to 103.9 mAh g^{-1} after 40 cycles. The capacity retention is only 89.9% of its initial discharge capacity. As for the $LiNi_{0.32}Mn_{0.33}Co_{0.33}Al_{0.01}O_2$, the initial capacity is 123.6 mAh g^{-1}, but the capacity retention after 40 cycles is improved to 97.0%. One reason for the capacity fading of layered materials is due to the instability of the delithiated electrode surface. It has been suggested that doping of Al could reduce the reactivity of the cathode toward electrolyte oxidation [25]. The result could be proved by the following EIS tests. Another possible reason is that the bonding energy of Al–O is much stronger than that of Ni–O, therefore, Al-doping could make the crystal structure of cathode material more stable [26–28]. Moreover, there is less Ni^{2+} ions occupy the Li^+ layers for the doped sample which could stabilize the layered structure during cycling.

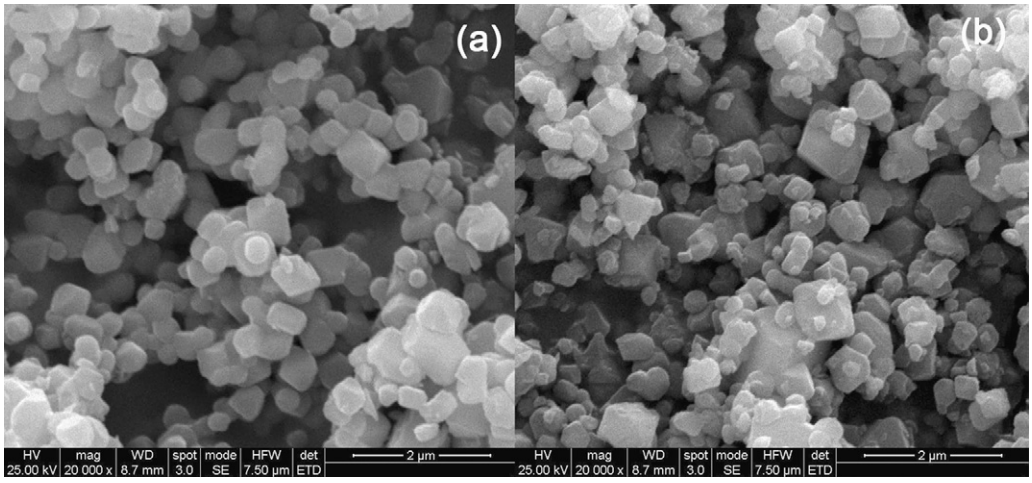

Fig. 2. SEM images of $LiNi_{0.33-x}Mn_{0.33}Co_{0.33}Al_xO_2$ powders: (a) $x = 0$, (b) $x = 0.01$.

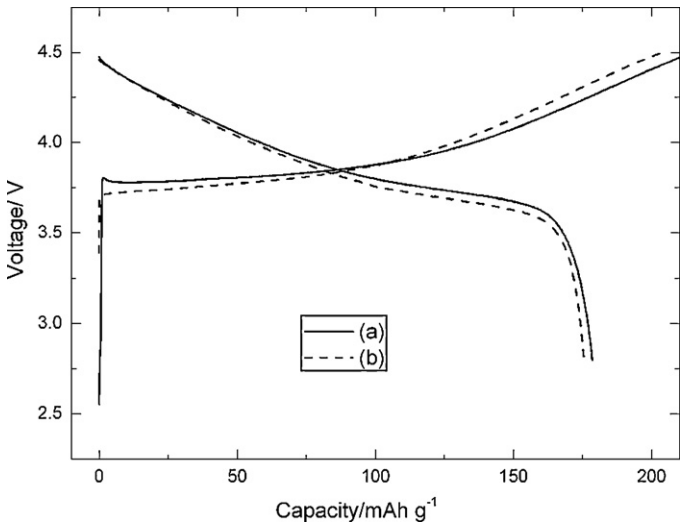

Fig. 3. The initial charge–discharge curves of $LiNi_{0.33-x}Mn_{0.33}Co_{0.33}Al_xO_2$ powders: (a) $x = 0$ and (b) $x = 0.01$.

Rate capability test also demonstrated the advantages of $LiNi_{0.32}Mn_{0.33}Co_{0.33}Al_{0.01}O_2$ as shown in Fig. 5. The cells were charged at 0.2 C and discharged at 0.2, 1.0, 2.0, 3.0, 4.0 and 5.0 C, respectively. The discharge capacity of $LiNi_{0.33}Mn_{0.33}Co_{0.33}O_2$ drops dramatically with increasing current densities: reaches to 115.4, 90.1 and 78.8 mAh g^{-1} at 2.0, 4.0 and 5.0 C, which are only 69.7, 54.3 and 47.5% of the capacity of 165.8 mAh g^{-1} at 0.2 C, respectively. However, the rate capability is improved significantly by Al-doping. The $LiNi_{0.32}Mn_{0.33}Co_{0.33}Al_{0.01}O_2$ presented a capacity of 127.3, 114.2 and 108.4 mAh g^{-1} at 2.0, 4.0 and 5.0 C, corresponding to 80.0, 71.8 and 68.1% of its capacity at 0.2 C (159.1 mAh g^{-1}). In brief, the rate capability of $LiNi_{0.32}Mn_{0.33}Co_{0.33}Al_{0.01}O_2$ is much better than that of $LiNi_{0.33}Mn_{0.33}Co_{0.33}O_2$. This relates to larger lattice parameter of *c* caused by Al-doping. The increasing of *c* could result in easy mobility of Li^+ ions in the layered oxide compound to enhance rate capability.

3.3. Cyclic voltammetry (CV)

Cyclic voltammograms for $LiNi_{0.33-x}Mn_{0.33}Co_{0.33}Al_xO_2$ electrodes are shown in Fig. 6. It could see that the difference of the curves on the first cycle and the subsequent cycles is obvious for the undoped sample. However, the intensity of the cyclic voltam-

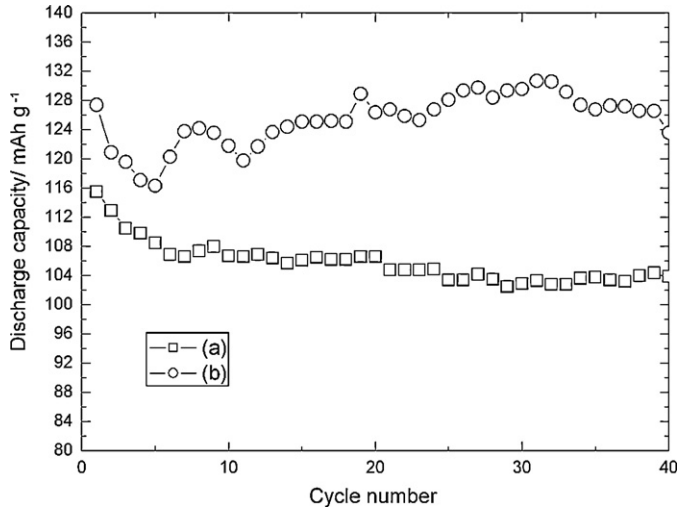

Fig. 4. Selected charge–discharge curves of $LiNi_{0.33-x}Mn_{0.33}Co_{0.33}Al_xO_2$ powders obtained during cycling at 0.2 C: (a) $x = 0$ and (b) $x = 0.01$.

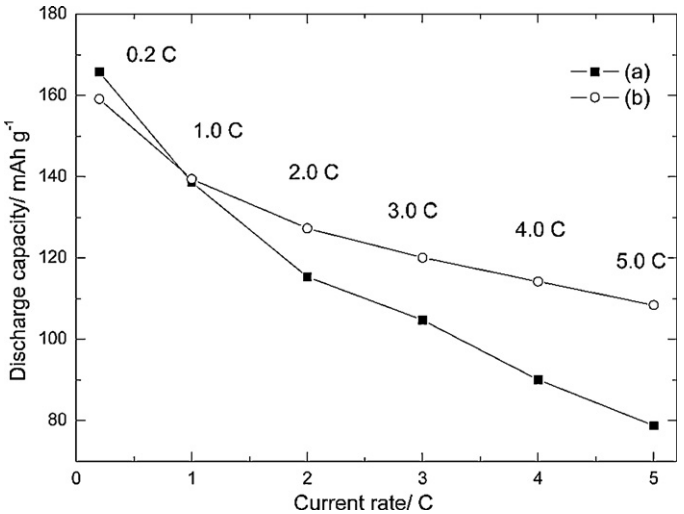

Fig. 5. Rate capability of $LiNi_{0.33-x}Mn_{0.33}Co_{0.33}Al_xO_2$ cells at different current density: (a) $x = 0$ and (b) $x = 0.01$.

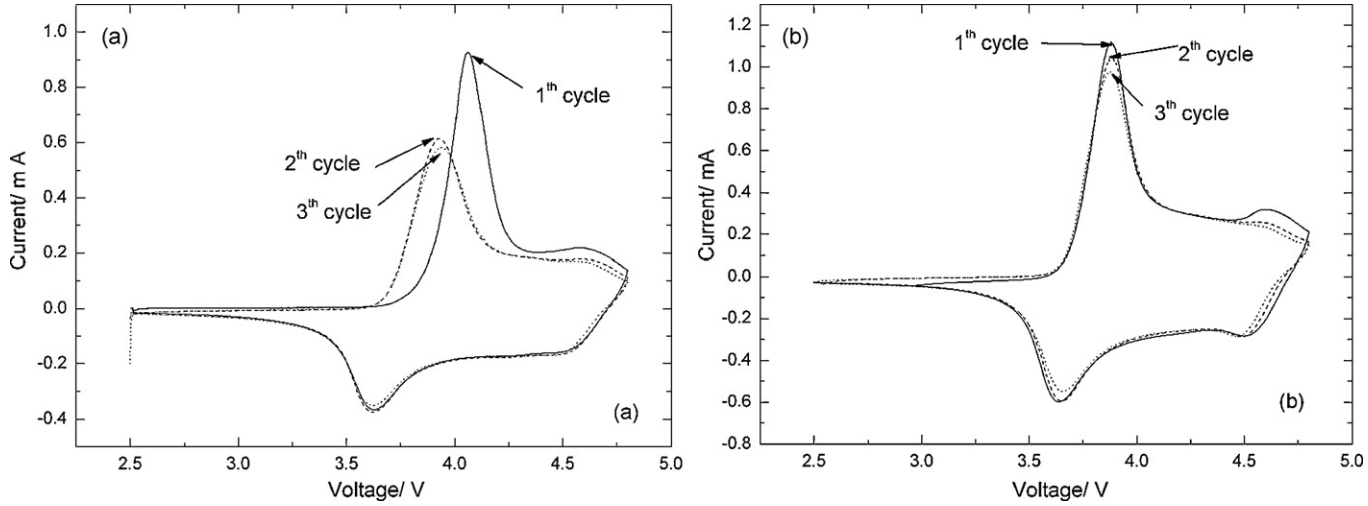

Fig. 6. Cyclic voltammogram of $LiNi_{0.33-x}Mn_{0.33}Co_{0.33}Al_xO_2$ cells at the scan rate of 0.1 mV s^{-1}: (a) $x = 0$ and (b) $x = 0.01$.

mogram curves almost unchanged after doping which means the irreversible loss of capacity and activation of the electrode on contact with the electrolyte are greatly suppressed. It could see that the cathodic peaks for the undoped one of the first cycle center at 4.06 and 4.61 V which correspond to the Ni^{2+}/Ni^{4+} and Co^{3+}/Co^{4+}. And the corresponding anodic peaks shift to 3.64 and 4.54 V, respectively. In the meantime, the cathodic peaks of the $LiNi_{0.32}Mn_{0.33}Co_{0.33}Al_{0.01}O_2$ center at 3.88 and 4.61 V, and the anodic peaks at 3.65 and 4.52 V. Obviously, the potential difference of the major peak corresponding to the Ni^{2+}/Ni^{4+} for the doped one is 0.23 V which is greatly depressed when compared to that of the $LiNi_{0.33}Mn_{0.33}Co_{0.33}O_2$ (about 0.42 V). It is well known that the bigger the potential difference between intercalate and deintercalate lithium-ions, the stronger the electrode polarization is. As doping reduces the difference of the position between oxidation and reduction peaks which indicates the better reversibility of Li^+ ions during intercalating/deintercalating in $LiNi_{0.32}Mn_{0.33}Co_{0.33}Al_{0.01}O_2$ materials which, in turn, ensures reduced capacity fade during cycling [29].

3.4. Electrochemical impedance spectroscopy (EIS)

In this study, EIS tests were performed on the electrodes at charged state (to 4.5 V). Fig. 7 illustrates the EIS profiles of $LiNi_{0.33-x}Mn_{0.33}Co_{0.33}Al_xO_2$ cells before and after 40 cycles at 1.0 C. The impedance spectra consist of two semicircles in the high and intermediate-frequency ranges and followed by an inclined straight line at the low frequency range. The high frequency semicircle related the Li^+ ion migration resistance (R_{sei}) through the solid electrolyte interface layer formed on the surface of the electrode by the reaction between the lithium metal oxide and electrolyte; the intermediate-frequency semicircle is attributed to the charge transfer resistance (R_{ct}) in the cathode–electrolyte interface. And the inclined straight line at the low frequency end is attributed to Warburg impedance that is associated with Li^+ diffusion through the cathode [30–32].

From the Fig. 7a and b, it could also see that the R_{sei} of $LiNi_{0.33}Mn_{0.33}Co_{0.33}O_2$ is similar to that of the Al-doped one when the first charged to 4.5 V, which means the solid electrolyte interface layer formed on the surface of the electrode has no great difference. However, the R_{ct} of the doped sample is significantly smaller than that of the undoped one. One interpretation is that it is easier for Li^+ intercalate and deintercalate when lattice parameters c becomes larger after doping Al ions. After 40 cycles, R_{ct} of both samples are significantly grown, while the increase of R_{sei} are very small. This result indicates that the increase in resistance of $LiNi_{1/3}Mn_{1/3}Co_{1/3}O_2$ is dominated by increase in the charge transfer resistance. The diameter of second semicircle of $LiNi_{0.33}Mn_{0.33}Co_{0.33}O_2$ cathode is 58.9 Ω at first cycle then enlarges drastically to 177.2 Ω at 40th cycle. By contrast, the diameter

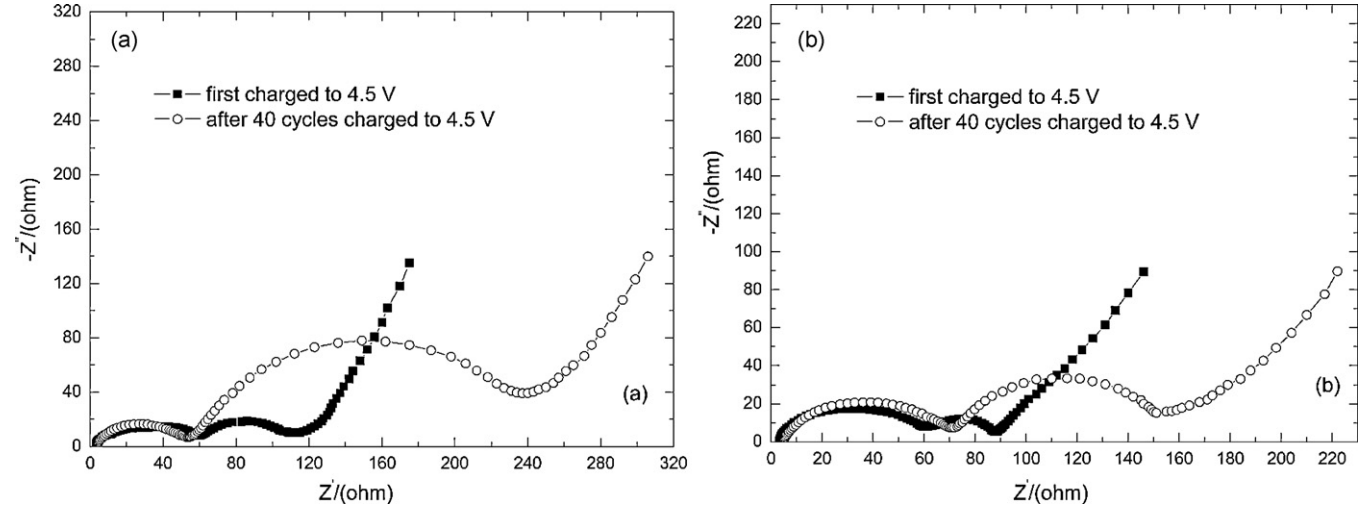

Fig. 7. Impedance spectra (Z' vs. Z'') of $LiNi_{0.33-x}Mn_{0.33}Co_{0.33}Al_xO_2$ cells: (a) $x = 0$ and (b) $x = 0.01$.

of second semicircle of $LiNi_{0.32}Mn_{0.33}Co_{0.33}Al_{0.01}O_2$ cathode only increases from 27.8 Ω at first cycle to 80.8 Ω at 40th cycle. It shows that Al-doping has an effective effect on restraining the increasing of charge transfer impedance of cathode during cycling. Small impedance is favorable for the intercalation and de-intercalation of lithium-ions during the charge and discharge process. Hence, the EIS test confirms the improvement of electrochemical properties.

4. Conclusions

A novel layered $LiNi_{0.32}Mn_{0.33}Co_{0.33}Al_{0.01}O_2$ was successfully synthesized by sol–gel method. The structure, morphology and electrochemical properties of it were investigated in detail. The results show that Al^{3+} substitute for Ni^{2+} could increase the Li^+ diffusion coefficient in the lattice and decrease the cation mixing in Li layer without changing the phase composition and particle morphology. Although the discharge capacity of $LiNi_{0.32}Mn_{0.33}Co_{0.33}Al_{0.01}O_2$ is a little smaller than that of $LiNi_{0.33}Mn_{0.33}Co_{0.33}O_2$, the cycling performance and rate capability of $LiNi_{0.32}Mn_{0.33}Co_{0.33}Al_{0.01}O_2$ are much better than $LiNi_{0.33}Mn_{0.33}Co_{0.33}O_2$. CV results show that there is a better reversibility of Li^+ ions during intercalating/deintercalating in the $LiNi_{0.32}Mn_{0.33}Co_{0.33}Al_{0.01}O_2$ material. EIS results reveal that the increasing of the charge transfer impedance of the $LiNi_{0.32}Mn_{0.33}Co_{0.33}Al_{0.01}O_2$ during cycling is greatly restrained.

Acknowledgements

This work was financially supported by the National 973 program (Contract Nos. 2002CB211800 and 2009CB220100), National High-tech 863 key program (Contract Nos. 2006AA11A165) and BIT Basic Research Fund (Contract Nos. 20070542004).

References

[1] T. Ohzuku, Y. Makimura, Chem. Lett. (2001) 642.
[2] K.M. Shaju, G.V. Subba Rao, B.V.R. Chowdari, Electrochim. Acta 48 (2002) 145.
[3] J.-M. Kim, H.-T. Chung, Electrochim. Acta 49 (2004) 3573.
[4] S.H. Park, C.S. Yoon, S.G. Kang, H.-S. Kim, S.-I. Moon, Y.-K. Sun, Electrochim. Acta 49 (2004) 557.
[5] M.-H. Lee, Y.-J. Kang, S.-T. Myung, Y.-K. Sun, Electrochim. Acta 50 (2004) 939.
[6] G.-H. Kim, S.-T. Myung, H.-S. Kim, Y.-K. Sun, Electrochim. Acta 51 (2006) 2447.
[7] S.-H. Kang, J. Kim, M.E. Stoll, D. Abraham, Y.K. Sun, K. Amine, J. Power Sources 112 (2002) 41.
[8] Y.-K. Lin, C.-H. Lu, H.-C. Wu, M.-H. Yang, J. Power Sources 146 (2005) 594.
[9] G.T.K. Fey, J.G. Chen, V. Subramanian, T. Osaka, J. Power Sources 112 (2002) 384.
[10] H. Li, G. Chen, B. Zhang, J. Xiu, Solid Sate Commun. 146 (2008) 115.
[11] P.-Y. Liao, J.-G. Duh, H.-S. Sheu, J. Power Sources 183 (2008) 766.
[12] W. Li, J.N. Reimers, J.R. Dahn, Solid State Ionics 67 (1993) 123.
[13] J.A. Dean, Lange's Handbook of Chemistry, 15th ed., McGraw-Hill Inc., USA, 1999.
[14] M. Guilmard, A. Rougier, M. Grune, L. Croguennec, C. Delmas, J. Power Sources 115 (2003) 305.
[15] S. Castro-Carcia, A. Castro-Couceiro, M.A. Senaris-Rodriguez, F. Soulette, C. Julien, Solid Sate Ionics 156 (2003) 15.
[16] S.-T. Myung, N. Kumagai, S. Komaba, H.-T. Chung, Solid State Ionics 139 (2001) 47.
[17] H. Huang, G.V. Subba Rao, B.V.R. Chowdari, J. Power Sources 81–82 (1999) 690.
[18] S.W. Oh, S.H. Park, C.-W. Park, Y.-K. Sun, Solid State Ionics 171 (2004) 167.
[19] Y.M. Choi, S. Pyun II, S.I. Moon, Solid State Ionics 89 (1996) 43.
[20] T. Ohzuku, A. Ueda, M. Nagayama, J. Electrochem. Soc. 140 (1993) 1862.
[21] T. Ohzuku, A. Ueda, M. Nagayama, Y. Iwakoshi, H. Komori, Eletrochem. Acta 38 (1993) 1159.
[22] S.-T. Myung, S. Komaba, N. Hirosaki, K. Hosoya, N. Kumagai, J. Power Sources 146 (2005) 645.
[23] C. Delmas, M. Menetrier, L. Croguennec, I. Saadoune, A. Rougier, C. Pouillerie, G. Prado, M. Grune, L. Fournes, Electrochim. Acta 45 (1999) 243.
[24] I. Saadoune, C. Delmas, J. Mater. Chem. 6 (1996) 193.
[25] T. Ohzuku, A. Ueda, M. Kouguchi, J. Electrochem. Soc. 142 (1995) 4033.
[26] S.H. Park, Y.K. Sun, J. Power Sources 119–121 (2003) 161.
[27] C.Q. Xu, Y.W. Tian, Y.C. Zhai, L.Y. Liu, Mater. Chem. Phys. 98 (2006) 532.
[28] D. Song, H. Ikuta, T. Uchida, M. Wakihara, Solid State Ionics 117 (1999) 151.
[29] G.G. Amatucci, M.M. Tarascon, L.C. Klein, Solid State Ionics 83 (1996) 167.
[30] G.T.-K. Fey, P. Muralidharan, C.-Z. Lu, Y.-D. Cho, Electrochim. Acta 51 (2006) 4850.
[31] M.D. Levi, K. Gamolsky, D. Aurbach, U. Heider, R. Oesten, Electrochim. Acta 45 (2000) 1781.
[32] Z.R. Zhang, H.S. Liu, Z.L. Gong, Y. Yang, J. Power Sources 129 (2004) 101.